

OMAE2009-79391

MOTION BEHAVIOUR OF A NEW OFFSHORE LNG TRANSFER SYSTEM AT HARSH OPERATIONAL CONDITIONS

Günther F. Clauss

Naval Architecture & Ocean Engineering
Technical University of Berlin
Germany
Email: clauss@naoe.tu-berlin.de

Florian Sprenger*

Naval Architecture & Ocean Eng.
Technical University of Berlin
Germany
Email: f.sprenger@naoe.tu-berlin.de

Daniel Testa*

Naval Architecture & Ocean Eng.
Technical University of Berlin
Germany
Email: testa@naoe.tu-berlin.de

Sven Hoog

IMPac Offshore Engineering
Hamburg, Germany
Email: sven.hoog@impac.de

Roland Huhn

IMPac Offshore Engineering
Hamburg, Germany
Email: roland.huhn@impac.de

ABSTRACT

Today, the demand of natural gas from offshore fields is on a high level and still increasing. Floating turret moored terminals receive gas directly from the field via risers and liquefaction is achieved by on-board processing plants. The LNG (liquefied natural gas) is transferred to periodically operating shuttle carriers for onshore supply.

This paper presents an innovative offshore LNG transfer system, based on newly developed flexible cryogenic pipes of 16" inner diameter, which allow fast loading/offloading procedures in tandem configuration (see Fig. 1), even in harsh environmental conditions.

The motion characteristics of the proposed concept are investigated in detail by the potential theory programmes WAMIT and ANSYS AQWA, respectively, with the focus on the dynamic behaviour of the multi-body system in waves. Each vessel is generating its own radiation and diffraction wave field affecting the motions of the adjacent vessels and vice versa. Results from calculations in the frequency and time domain are compared and show good agreement. Tolerable relative motions between terminal and carrier are limited by maximum torsion and bending of the flexible transfer pipe.

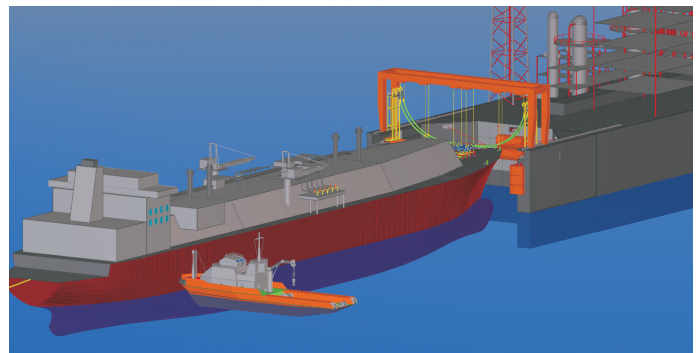


Figure 1. IMPRESSION OF THE NEW OFFSHORE LNG TRANSFER SYSTEM WITH A CARRIER COUPLED TO THE TERMINAL FOR LOADING

Based on given limiting parameters, the operational range of the system and the annual expected downtime is exemplarily calculated for a location in the north sea. Finally, second-order forces — induced by drift motions — on the mooring lines between carrier and terminal are presented as time series for a three-hour sea state.

*Address all correspondence to these authors.

INTRODUCTION

For several decades, natural gas was merely a byproduct of oil production. Today, its importance as energy source is still growing. Most natural gas is produced from offshore fields, with associated problems of transportation to further onshore processing. The deployment of LNG tank ships (Liquefied Natural Gas) is an alternative to pipelines with increasing significance [1]. In order to achieve economically reasonable transportation, the natural gas (mostly methane) is cooled down to -160°C , whereby it is liquefied and reduced to $1/600^{\text{th}}$ of its original volume.

For safe storage of LNG, specially insulated loading pipes and tanks are required. It has to be distinguished between two types of tanks: octahedral membrane tanks (see Fig. 2, top left) and spherical 'MOSS' tanks (see Fig. 2, top right). Until to-



Figure 2. LNG-CARRIER WITH MEMBRANE TANKS (TOP LEFT), AND SPHERICAL 'MOSS' TANKS (TOP RIGHT), IMPRESSIONS OF OFFSHORE LOADING IN SIDE-BY-SIDE (BOTTOM LEFT) AND TANDEM CONFIGURATION (BOTTOM RIGHT)

day, only one offshore LNG transfer system — based on the emergency unloading technology — was tested in calm water conditions and side-by-side configuration using 8" non-insulated composite hoses [2]. However, the increasing loading capacity of currently built LNG carriers (up to 260.000 m^3) creates a new market for fast and safe loading/offloading concepts — i.e. larger pipe diameters and transfer operations in rough seas [3].

Offshore terminal designs for production and processing of natural gas are typically fixed at a certain location by turret mooring and transfer the liquefied gas to periodically operating shuttle tankers in side-by-side configuration (see Fig. 2, bottom left) [4], [5].

In the framework of the joint research project *Maritime Pipe Loading System 20"* (MPLS20), an innovative offshore transfer system between a turret moored terminal barge and a shuttle car-

rier in tandem configuration is developed [6]. *Brugg Pipe Systems* is designing a corrugated transfer pipe of 16" inner diameter for LNG loading/offloading — which is significantly exceeding currently existing pipe diameters and hence transfer rates. The work of *Nexans Industries* focusses on connection techniques, *IMPAC Offshore Engineering GmbH* is in authority of the approaching and handling system and *Technical University Berlin* is conducting model tests as well as numerical simulations in order to analyse the hydrodynamical characteristics of the coupled system.

In the following sections, the system is analysed in tandem configuration (see Fig. 2, bottom right) at a water depth of $d = 100\text{ m}$. The shuttle carrier is towed between special mooring wings of 40 m length at the stern of the terminal, and is moored by six hawsers at a distance of 10 m. A loading frame is moved directly above the connectors on board of the tanker and four specially developed 16" transfer pipes are connected — three to load the tanks of the carrier and one additional pipe for vapor return.

MOTION ANALYSIS

For ensuring safe loading and offloading procedures, detailed knowledge on the motion characteristics of the carrier and the terminal in tandem configuration is required. Due to the turret mooring of the terminal, the entire system is weathervaning according to the angle of attack β of the superimposed environmental loads from waves, current and wind (see Fig. 3). As an idealized case, head waves ($\beta = 180^{\circ}$) are exclusively

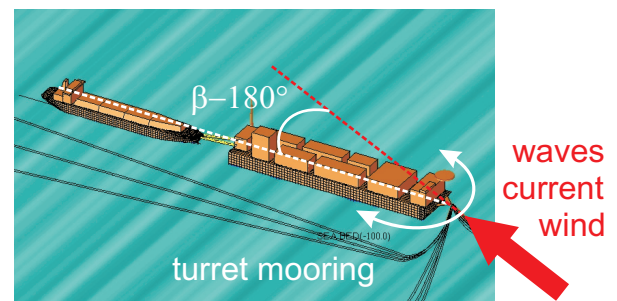


Figure 3. WEATHERVANING EFFECTS DUE TO THE TURRET MOORING OF THE SYSTEM

considered in the following investigations. The focus lies on the transfer configuration with completely filled cargo tanks and the respective distance of 10 m between terminal stern and carrier bow is applied for all computations. The main dimensions of the terminal and the carrier are shown in Tab. 1. The carrier features four tanks of equal size with a total loading ca-

Parameter	Terminal	Carrier
Length over all	360 m (+ 40 m mooring wings)	285 m
Breadth	65 m	42 m
Draught	12 m	12 m
Height	33 m	26 m
Displacement	275.087 m ³	103.921 m ³

Table 1. MAIN DIMENSIONS OF THE LNG CARRIER AND THE TERMINAL

capacity of 138.000 m³. Both hulls are discretised for frequency-domain analyses with WAMIT (Wave Analysis at Massachusetts Institute of Technology [7], 3600 panels in total) and for time-domain analyses with ANSYS AQWA (2900 panels in total). WAMIT is widely accepted as a reliable tool for hydrodynamic analyses in offshore technology and proved to be suitable for multi-body problems [8]. Both programme codes are based on potential theory, i.e. on the fulfillment of Laplace's Equation

$$\Delta\Phi = \frac{\partial^2\Phi}{\partial x^2} + \frac{\partial^2\Phi}{\partial y^2} + \frac{\partial^2\Phi}{\partial z^2} = 0 \quad (1)$$

Since the hydrodynamic problem is of three-dimensional nature and comprises two bodies, a total of 15 potentials has to be determined

$$\Phi = \Phi_0 + \Phi_{7,k} + \sum_{j=1}^6 \Phi_{j,k} \quad (2)$$

where k is the number of the respective body and the degrees of freedom are denoted by j . Φ_0 is the potential of the incident wave, $\Phi_{7,k}$ the scattering potential of the body and $\Phi_{j,k}$ the radiation potentials for body motions in six degrees of freedom.

In addition to the analysis of wave-induced body motions with WAMIT, ANSYS AQWA offers the possibility of including marine currents as well as wind at different velocities.

Global Motion Behaviour

At sea states from $\beta = 180^\circ$, the motion behaviour of the hydrodynamically coupled bodies is characterized by the RAOs (Response Amplitude Operator) for surge, heave and pitch:

$$H_j(\omega) = \frac{s_{ja}(\omega)}{\zeta_a(\omega)} e^{i\varepsilon_j(\omega)} \quad \text{with } \begin{array}{l} j = 1 \text{ for surge} \\ j = 3 \text{ for heave} \\ j = 5 \text{ for pitch,} \end{array} \quad (3)$$

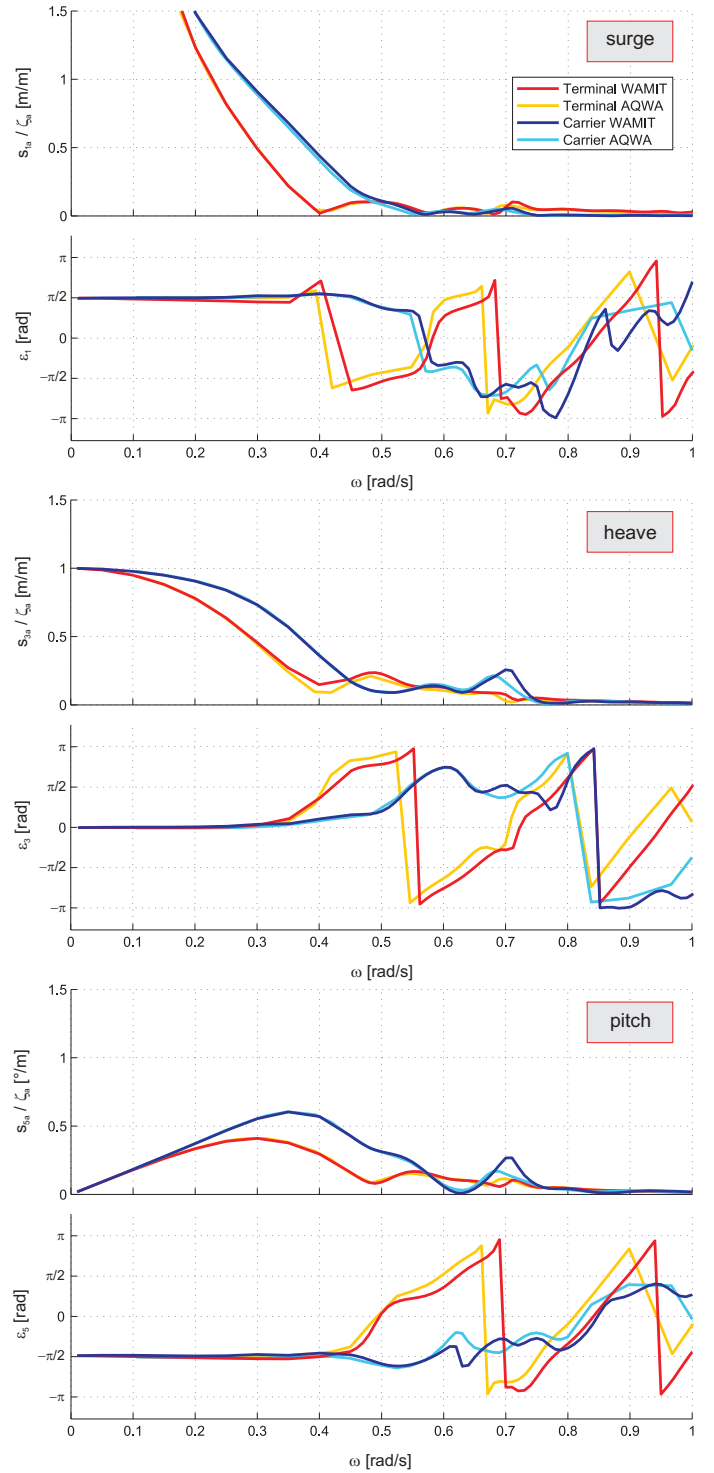


Figure 4. COMPARISON OF THE SURGE, HEAVE AND PITCH RAOs ($\beta = 180^\circ$) FOR THE TERMINAL AND THE CARRIER IN LOADING/OFFLOADING CONFIGURATION OBTAINED BY WAMIT AND ANSYS AQWA

where ω is the angular wave frequency, ζ_a is the wave amplitude, s_{ja} is the amplitude of the respective body motion and ε_j is the corresponding phase angle. The absolute value of this complex number is obtained by $|H_j(\omega)|$ whereas the phase shift is calculated by

$$\varepsilon_j(\omega) = \tan^{-1} \left(\frac{\Im(H_j(\omega))}{\Re(H_j(\omega))} \right). \quad (4)$$

Fig. 4 shows the absolute values and phase angles of surge, heave and pitch RAOs for the carrier and the terminal. The comparison of results from WAMIT and ANSYS AQWA shows a good overall agreement, especially concerning the absolute values. The same applies for the phase angles, with some slight deviations occurring for high frequencies — i.e. short waves. Both, the carrier and the terminal follow the wave contour in very long waves and perform large surge motions with 90° phase shift (largest deflections at the zero crossings of the waves) until the wave length becomes smaller than their hull length. Due to the restricted water depth ($d = 100$ m), the surge RAOs converge to infinity in very long waves since the horizontal semi-major axis of the particle orbital paths $\zeta_a \cosh(k(z+d))/\sinh(kd)$ is growing with decreasing wave numbers k . The absolute value of the heave motion converges to one meter heave amplitude per meter wave amplitude without phase shift for very long waves, where both bodies follow the surface elevation like a floating cork. For shorter waves, heave motions are continuously decreasing. However, a local maximum for the carrier motions of 0.26 m per meter wave amplitude can be observed at $\omega \approx 0.7$ rad/s. The pitch motions converge to zero in very long waves and increase with -90° phase shift (largest pitch angles at zero crossings of the waves — i.e. on the wave slope) to a global maximum of 0.6° per meter wave amplitude at $\omega = 0.35$ rad/s for the carrier and 0.41° per meter wave amplitude at $\omega = 0.3$ rad/s for the terminal. Also, a local maximum of 0.27° per meter wave amplitude at $\omega \approx 0.7$ rad/s can be observed for the carrier pitch motions.

Relative Motions

For the design of the offshore transfer concept, the most critical property that has to be assessed in detail is the relative motion between the LNG carrier and the terminal barge in dependency of the environmental conditions. Considering head seas ($\beta = 180^\circ$) exclusively, one point per body is chosen to investigate the relative motion characteristics. First, two new complex RAOs ($H_{x,j}$ and $H_{z,j}$) for each point have to be calculated by the following procedure

$$\begin{bmatrix} H_{x,j}(\omega) \\ 0 \\ H_{z,j}(\omega) \end{bmatrix} = \begin{bmatrix} H_{1,j}(\omega) \\ 0 \\ H_{3,j}(\omega) \end{bmatrix} + \begin{bmatrix} 0 \\ H_{5,j}(\omega) \\ 0 \end{bmatrix} \times \begin{bmatrix} d_{x,j} \\ d_{y,j} \\ d_{z,j} \end{bmatrix} \quad (5)$$

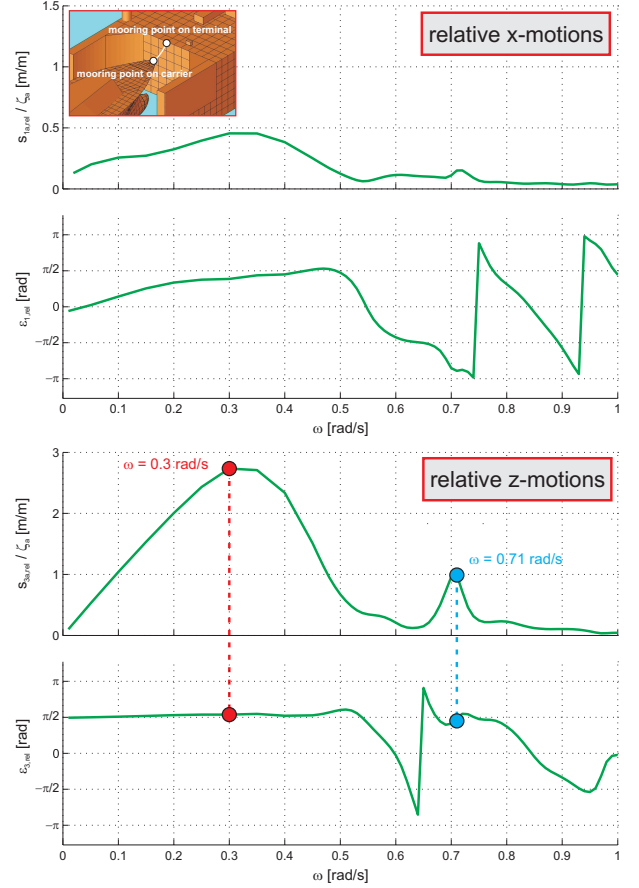


Figure 5. ABSOLUTE VALUES AND PHASES OF RAOs OF RELATIVE X- AND Z-MOTIONS FOR THE MOORING POINTS OF THE FORELINE

where the original translatory RAOs of each body are denoted by $H_{1,j}$ and $H_{3,j}$, the rotatory RAOs by $H_{5,j}$ and the distance between the body fixed coordinate systems and the points of interest by $d_{x,j}$, $d_{y,j}$ and $d_{z,j}$. In order to obtain the relative motions between the two points, the difference of the RAOs for x -motions and z -motions is calculated

$$\begin{aligned} H_{x,rel}(\omega) &= H_{x,1}(\omega) - H_{x,2}(\omega) \\ H_{z,rel}(\omega) &= H_{z,1}(\omega) - H_{z,2}(\omega) \end{aligned} \quad (6)$$

For the subsequent calculations, the mooring points of the nose line between carrier and terminal are chosen. Since these are the points of greatest distance to the centres of rotation (bow of the tanker, stern of the terminal), they will experience the highest motions. Fig. 5 shows the RAOs of the relative motions in x - and z -direction. The relative x -motions converge to zero for very long waves, i.e. both bodies follow the surface elevation with large absolute surge motions but no relative x -motions. The

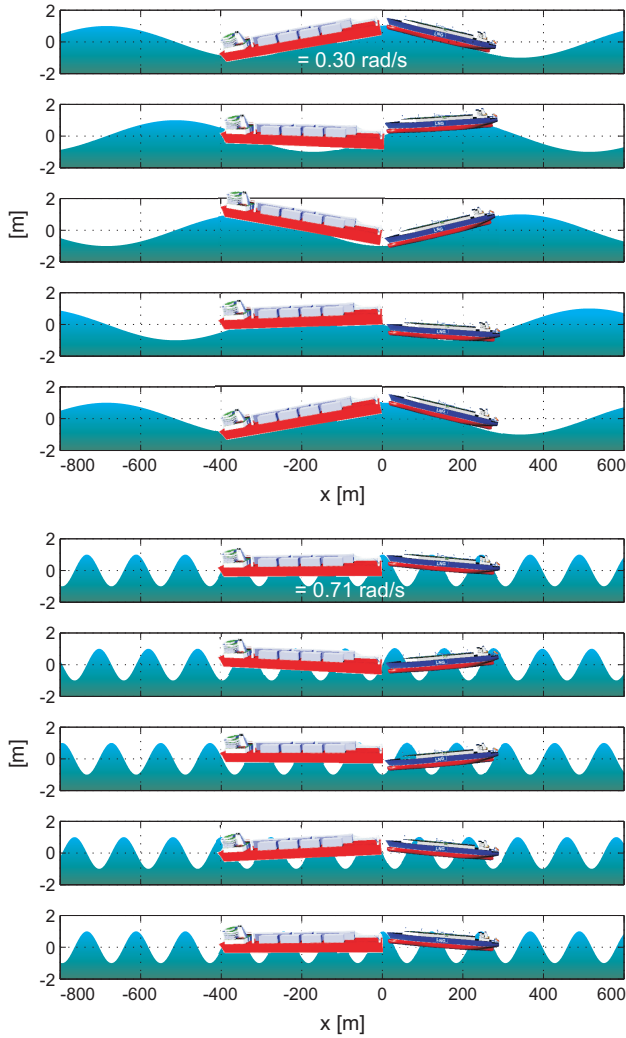


Figure 6. VISUALIZATION OF THE HEAVE AND PITCH MOTION OF THE LNG CARRIER AND THE TERMINAL BARGE IN REGULAR WAVES WITH $\omega = 0.30$ RAD/S (TOP) AND $\omega = 0.71$ RAD/S (BOTTOM)

global maximum of the relative x -motions is 0.45 m per meter wave amplitude at $\omega = 0.3$ rad/s with $\approx 90^\circ$ phase shift. For shorter waves, the relative motions are decreasing with a very small local maximum occurring at $\omega \approx 0.7$ rad/s.

In the z -direction, relative motions also converge to zero for very long waves. At $\omega = 0.30$ rad/s, the global maximum reaches 2.73 m relative motion per meter wave amplitude with a phase shift of 90° . At $\omega = 0.71$ rad/s, a local maximum of 0.99 m relative motion per meter wave amplitude is observed. The red and cyan markers indicate angular wave frequencies ($\omega = 0.30$ rad/s and $\omega = 0.71$ rad/s, respectively), for which the calculated heave and pitch motions of the carrier and the barge are exemplarily visualized at four different instances in Fig. 6.

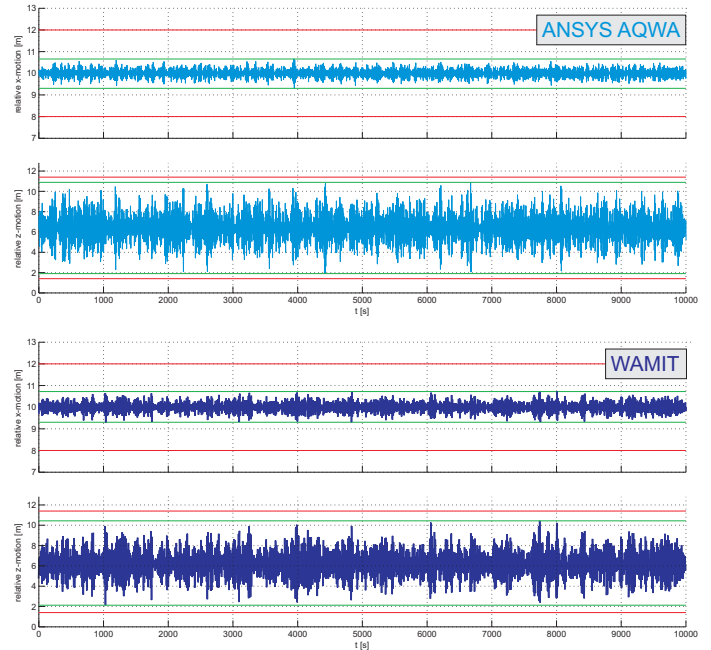


Figure 7. COMPARISON OF TIME SERIES OF RELATIVE X- AND Z-MOTIONS OBTAINED BY ANSYS AQWA (CYAN) AND WAMIT (DARK BLUE)

Please note that the impression of the terminal barge and the carrier is scaled correctly with respect to the wave length (x -axis) but not to the wave height (y -axis). In both regular sea states (each with $\zeta_a = 1$ m), the highest relative z -motions occur at the zero-crossing of the waves, visualizing the phase shift of 90° between relative motions and the surface elevation. For the longer wave with $\omega = 0.30$ rad/s, higher motions are observed — 2.73 m per meter wave amplitude compared to 0.99 m per meter wave amplitude for the short wave ($\omega = 0.71$ rad/s).

In order to compare the results of the frequency-domain analyses conducted with WAMIT to the time-domain results of ANSYS AQWA, inverse Fast-Fourier-Transformations (IFFT) with random phases are applied. In Fig. 7, the respective time series for an irregular sea state (JONSWAP, $\gamma = 3.3$, $H_s = 5.5$ m, $\omega_p = 0.5$ rad/s) of approx. 3 hours are shown. The motions in both directions feature an offset due to the horizontal and vertical distances of the mooring points of the nose line on the terminal and the carrier ($\Delta x = 10$ m, $\Delta z = 6.4$ m). The maximum tolerable relative motion amplitudes are indicated by red lines (± 2 m in x -direction and ± 5 m in z -direction). Green lines show the maximum occurring motion amplitudes, which are within the tolerable limits for all cases. Since the irregular sea states generated by both programme codes feature random phases, maximum motion values of the time series are compared. The agreement for the maximum positive relative x - and z -motion as well as the

maximum negative relative x - and z -motion is very good, with a maximum deviation of 9.79 % (see Tab. 2).

Parameter	WAMIT	ANSYS AQWA
$(s_{xa,rel})_{max}$	+0.71 m / -0.78 m	+0.66 m / -0.70 m
$(s_{za,rel})_{max}$	+4.40 m / -4.39 m	+4.49 m / -4.50 m

Table 2. COMPARISON OF MAXIMUM RELATIVE MOTION AMPLITUDES

Operational Range of the Proposed Concept

On basis of the relative motion RAOs for the connection points of the transfer pipe, the operational range of the system — i.e. terminal and carrier in tandem configuration at a distance of 10 m (loading condition) — is determined. The location chosen for this exemplary investigation is a position in the North Sea ($55^\circ 0.00$ N, $6^\circ 20.00$ E).

At first, a range of JONSWAP spectra with varying zero-upcrossing-periods ($3 \text{ s} \leq T_0 \leq 12 \text{ s}$) is multiplied with the squared absolute value of the relative motion RAOs to obtain the response spectra of the relative motions

$$S_{sj,rel}(\omega, T_0) = S(\omega, T_0) |H_{j,rel}(\omega)|^2 \quad (7)$$

Calculating the significant double amplitudes

$$(2s_{j,rel})_s(T_0) = 4 \sqrt{\int_0^\infty S_{sj,rel}(\omega, T_0) d\omega} \quad (8)$$

and dividing them by the significant wave height, gives the significant RAOs for the relative motions. For predefined maximum tolerable relative motions (limited by the maximum bending radius of the loading pipe), tolerable significant wave heights are calculated in dependency of the zero-upcrossing-periods

$$(H_{s,tol})_{j,rel}(T_0) = (2s_{j,rel})_{s,tol} \frac{H_s}{(2s_{j,rel})_s(T_0)} \quad (9)$$

where the tolerable significant relative motion double amplitudes are given with $(2s_{x,rel})_{s,tol} = 2.15 \text{ m}$ and $(2s_{z,rel})_{s,tol} = 5.38 \text{ m}$ (assuming a statistical value of 1.86 for the ratio of tolerable maximum relative motions to tolerable significant relative motions). The data obtained can now be combined with a scatter diagram

for the chosen location in the North Sea [9] in order to determine the expected annual downtime. The entire calculation process is illustrated in Fig. 9 on page 7 and the result is an annual downtime of 0.73 % or 3 days.

Determination of Mooring Forces

The LNG carrier is towed between the mooring wings at the stern of the terminal and is moored in a symmetrical arrangement of six hawsers — two nose lines, two fore lines and two fore springs. The mooring lines are dimensioned to absorb second-order forces, resulting from non-linear drift motions of the system. First-order forces due to linear sea state-induced body motions are significantly higher and cannot be absorbed. The lines have to be veered and hauled up in order not to be damaged.

In Fig. 8, time series of the second-order forces on the fore spring (red), fore line (green) and the nose line (blue) are shown for irregular head seas ($\beta = 180^\circ$) based on a JONSWAP spectrum with $H_s = 5.5 \text{ m}$, $\omega_p = 0.5 \text{ rad/s}$ and $\gamma = 3.3$ calculated with ANSYS AQWA. Additionally, a constant current ($v_c = 1 \text{ m/s}$,

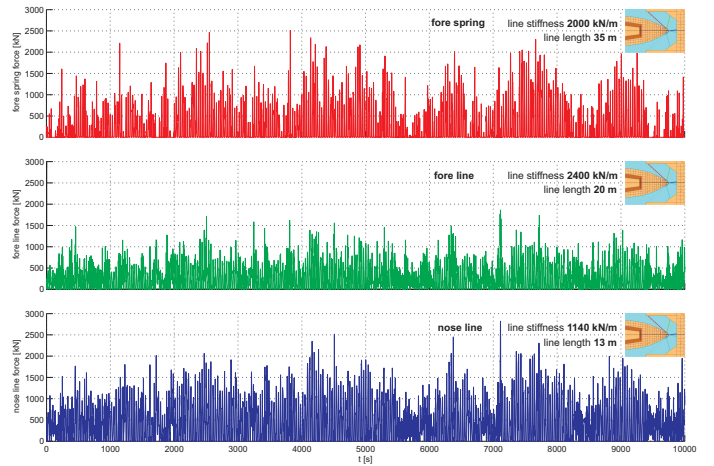


Figure 8. TIME SERIES OF THE SECOND-ORDER FORCES ON THE NOSE LINE (BLUE), FORE LINE (GREEN) AND FORE SPRING (RED) CALCULATED WITH ANSYS AQWA FOR AN IRREGULAR SEA STATE (JONSWAP, $H_s = 5.5 \text{ m}$, $\omega_p = 0.5 \text{ rad/s}$) AND $\beta = 180^\circ$

$\beta_c = 180^\circ$) and wind ($v_w = 30 \text{ m/s}$, $\beta_w = 180^\circ$) is assumed for the environmental conditions of the simulation. At the fore spring (length 35 m, stiffness 2000 kN/m), a maximum tensile force of 2511 kN is observed. The fore line (length 20 m, stiffness 2400 kN/m) has to absorb a maximum tensile force of 1861 kN, whereas the second-order loads on the nose line (length 13 m, stiffness 1140 kN/m) reach a peak value of 2821 kN for the chosen conditions.

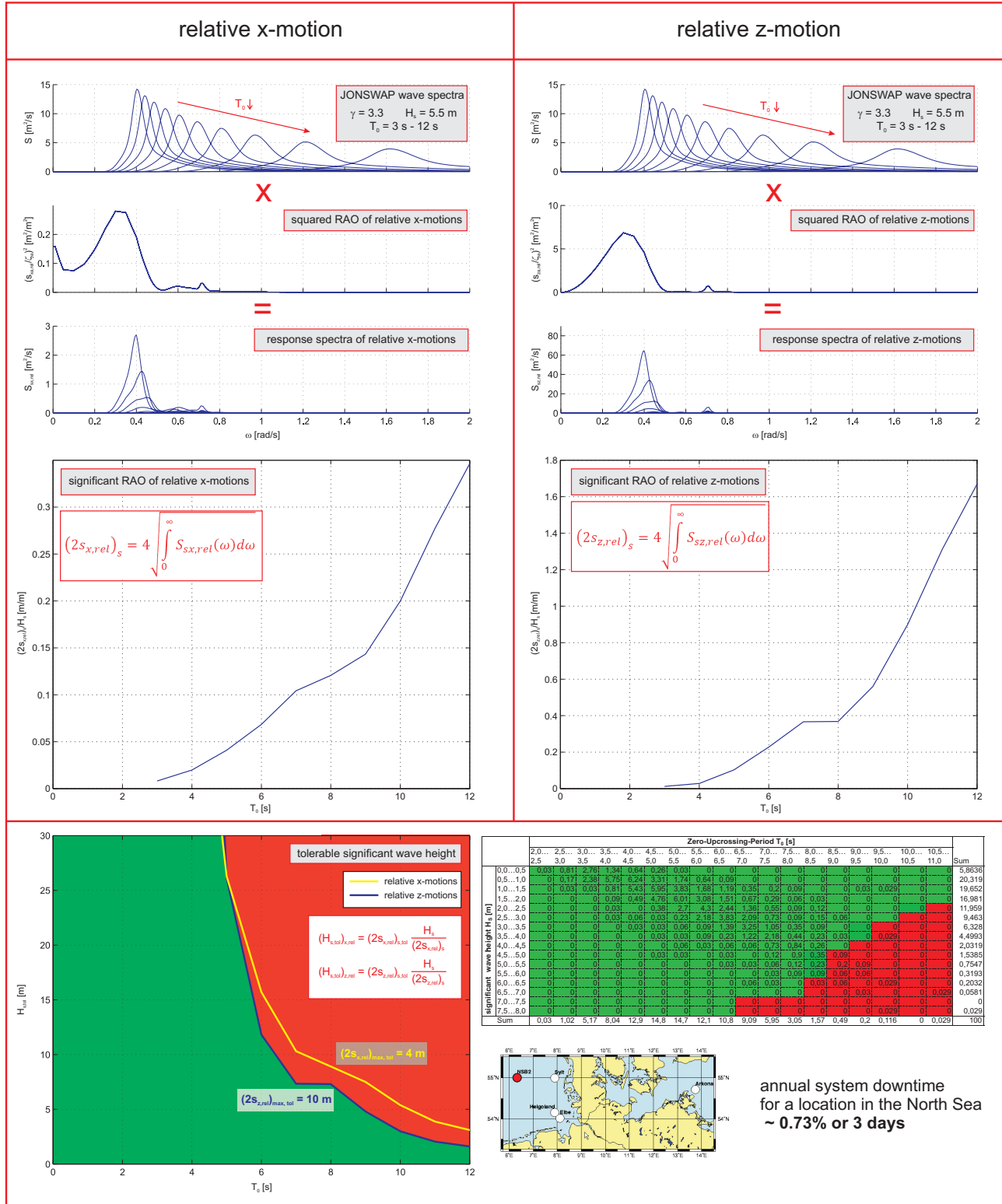


Figure 9. SCHEME OF THE CALCULATIONS OF THE OPERATIONAL RANGE BASED ON MAXIMUM TOLERABLE RELATIVE MOTIONS FOR THE CONNECTION POINTS OF THE TRANSFER PIPE

CONCLUSIONS

An innovative offshore LNG transfer system is introduced, where the shuttle carrier is towed between the mooring wings of a turret moored terminal to a distance of 10 m in tandem configuration. The liquefied gas is simultaneously transferred into four membrane tanks through three specially developed 16" pipes with one additional pipe for vapor return.

Various numerical analyses with the potential theory solvers WAMIT and ANSYS AQWA have been performed, where the interaction of the multi-body system due to diffraction and radiation effects is taken into account. Since the system takes advantage of the weathervaning effect, the results are presented for head seas exclusively (JONSWAP, $\gamma = 3.3$, $H_s = 5.5$ m, $\omega_p = 0.5$ rad/s, $\beta = 180^\circ$).

The surge, heave and pitch RAOs calculated for both bodies show good agreement of absolute values and phase angles. A maximum value of 0.6° per meter wave amplitude is observed for the carrier at $\omega = 0.35$ rad/s and of 0.41° per meter wave amplitude at $\omega = 0.3$ rad/s for the terminal. The graphs of all absolute values feature minor local maxima at $\omega \approx 0.7$ rad/s.

These local peaks are also existing in the RAOs of the relative x - and z -motions. The relative motions have been calculated with respect to the mooring points for the nose line on carrier and terminal. The calculations yield maximum values of 2.73 m per meter wave amplitude for the z -direction and 0.45 m per meter wave amplitude for the x -direction. The validation of time series from ANSYS AQWA simulations with results from WAMIT transferred into time-domain via IFFT show very good agreement with a maximum deviation of 9.79 %.

The investigation of relative motion RAOs for the connecting points of the transfer pipe are extended by spectral analyses, leading to an operational range for a location in the North Sea. For maximum tolerable relative x -motion amplitudes of ± 2 m and z -motion amplitudes of ± 5 m (limited by the maximum bending radius of the pipe), a downtime of 3 days per year is expected.

Finally, the second-order tensile forces on the mooring lines of the carrier are determined with ANSYS AQWA for the layout of nose lines, fore lines and fore springs.

The results presented emphasize that the proposed system with tandem configuration for offshore LNG transfer shows excellent seakeeping behaviour and the relative motions do not exceed tolerable values for the chosen sea states. Assuming a location in the North Sea, a marginal downtime of 3 days per year can be expected.

PERSPECTIVES

Since the superposition of waves, wind and marine currents from different directions can lead to a range of headings from 150° to 210° , further investigations have to be conducted. For these cases, the influence of the roll motion is no longer negli-

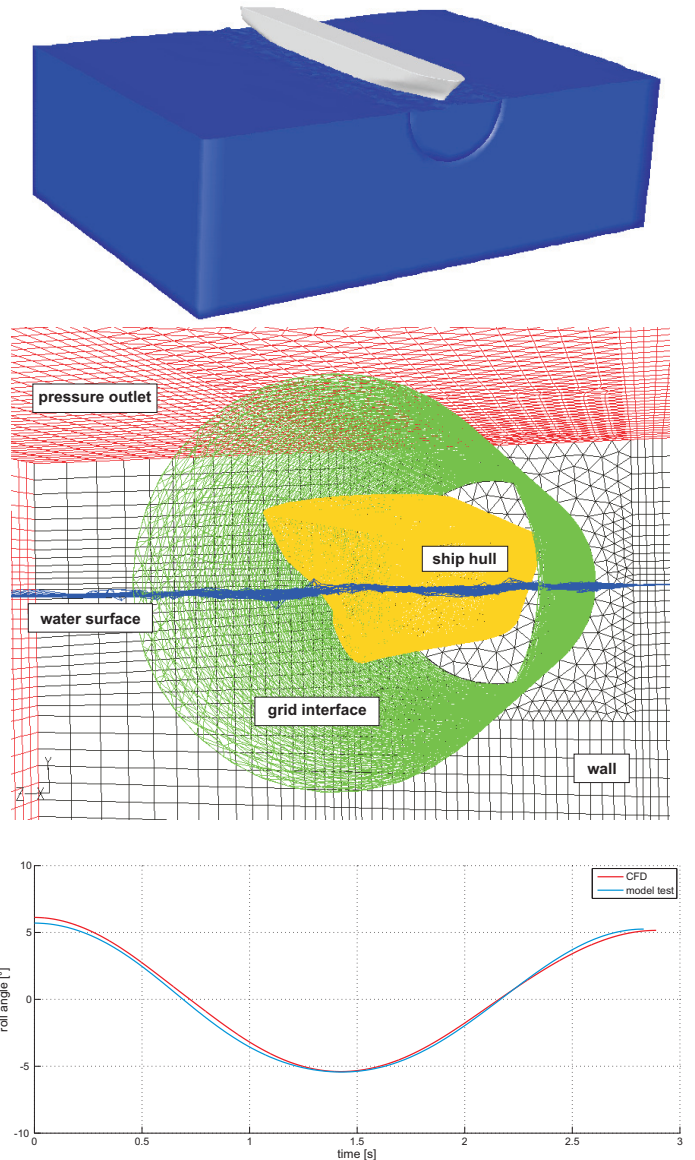


Figure 10. SCREENSHOT OF THE NUMERICAL SIMULATION WITH A CONTAINER VESSEL (TOP), GRID STRUCTURE WITH ROTATING INTERFACES (CENTRE), COMPARISON OF THE EXPERIMENTALLY (BLUE LINE) AND NUMERICALLY (RED LINE) DETERMINED VISCOUS ROLL DAMPING COEFFICIENTS

ble and requires detailed knowledge of viscous damping effects in order to obtain reasonable results. Experimental determination of viscous roll damping coefficients is state-of-the-art but is time consuming and requires exact procedures in order to obtain reliable results. For fast and efficient prediction of viscous roll damping, a three-dimensional numerical method based on a RANSE/VOF (Reynolds Averaged Navier-Stokes Equations,

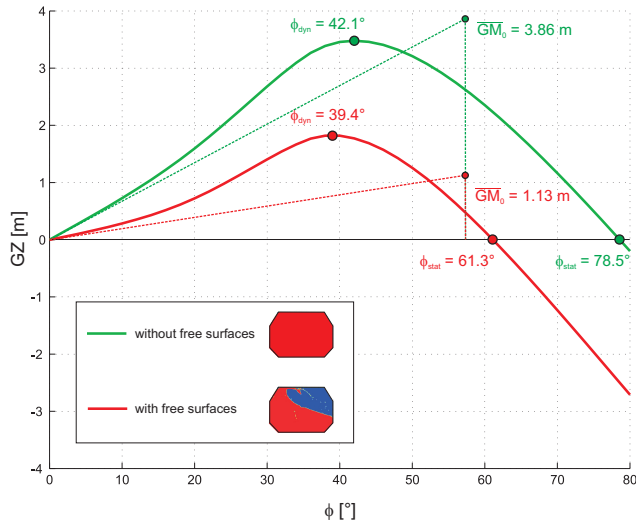


Figure 11. INITIAL STABILITY OF THE LNG CARRIER WITH (RED LINE) AND WITHOUT FREE FLUID SURFACES INSIDE THE CARGO TANKS (GREEN LINE)

Volume of Fluid — two phases) approach is developed. The model of a container vessel at scale 1:70 is used for validation. Fig. 10 (top) shows a three-dimensional view of the fluid domain discretized by approx. 425,000 cells. Roll motions of the hull are implemented by grid interfaces (see Fig. 10, centre) and special subroutines based on an explicit first order approach. As the resonance test shows good agreement with experimental data from model tests at the seakeeping basin of Technical University Berlin, this method will be used to calculate the viscous roll damping coefficients of the LNG carrier for further analyses.

Roll motions pose a threat for the carrier, in particular during the LNG transfer procedure. Since usually all four tanks are filled simultaneously, extremely large free fluid surfaces are developing for a certain time frame. The influence of free fluid surfaces on the initial intact stability of the LNG carrier is shown in Fig. 11. If all four tanks are partly filled, the metacentric height is reduced by 2.73 m to 1.13 m and the dynamic capsizing angle from 42.1° to 39.4° . The coupling of wave-induced tank sloshing with the ship motions is even more dangerous [10], [11] and will be analysed with numerical methods as well.

Also, extensive model tests with the system at scale 1:100 will be conducted in the seakeeping basin of Technical University Berlin.

ACKNOWLEDGMENT

The authors wish to express their gratitude to the German Federal Ministry of Economics and Technology (BMWi) and Project Management Jülich (PTJ) for funding the joint research project 'MPLS20 — Maritime Pipe Loading System 20' (FKZ

03SX240D), in particular to Dipl.-Ing. Barbara Grothkopp and Dipl.-Betriebswirtin Cornelia Bude for their excellent 'escort'. Furthermore, we want to thank our project partners 'Brugg Pipe Systems' and 'Nexans Industries' for their support. Many thanks also to our predecessors at Technical University Berlin, Dr.-Ing. Katja Jacobsen and Dr.-Ing. Robert Stück for their work on the project and to cand.-Ing. Achim Schmidt for his support in grid generation. Dipl.-Ing. Nils Otten kindly provided his roll damping model test results.

REFERENCES

- [1] Royal Institute of Naval Architects, 2006. "Gas Ships: Trends and Technology".
- [2] Cook, J., 2006. "Gulf Gateway Energy Bridge — The First Year of Operations and the Commercial and Operational Advantages of the Energy Bridge Technology". In Offshore Technology Conference. OTC 18396.
- [3] Frohne, C., Harten, F., Schipll, K., Steen, K. E., Haakonson, R., Eide, J., and Høvik, J., 2008. "Innovative Pipe System for Offshore LNG Transfer". In Offshore Technology Conference. OTC 19239.
- [4] Poldervaart, L., Oomen, H., and Ellis, J., 2006. "Offshore LNG Transfer: A Worldwide Review of Offloading Availability". OTC 18026.
- [5] Naciri, M., Waals, O., and de Wilde, J., 2007. "Time Domain Simulations of Side-by-Side Moored Vessels — Lessons Learnt from a Benchmark Test". In 26th International Conference on Offshore Mechanics and Arctic Engineering. OMAE2007-29756.
- [6] Hoog, S., Koch, H., Huhn, R., Frohne, C., Homann, J., Clauss, G., Sprenger, F., and Testa, D., 2009. "LNG Transfer in Harsh Environments — Introduction of a New Concept". In Offshore Technology Conference. OTC 19866.
- [7] Massachusetts Institute of Technology, 1994. *WAMIT Version 5.1 — A Radiation-Diffraction Panel Program For Wave-Body Interactions*. Userguide.
- [8] Jacobsen, K., and Clauss, G., 2006. "Time-Domain Simulations of Multi-Body Systems in Deterministic Wave Trains". In 25th International Conference on Offshore Mechanics and Arctic Engineering. OMAE2006-92348.
- [9] German Federal Maritime and Hydrographic Agency, 2005. Homepage of the German Federal Maritime and Hydrographic Agency. http://www.bsh.de/en/Marine_data/Observations/Sea_state.
- [10] Faltinsen, O., and Rognebakke, O., 2003. "Coupling of Sloshing and Ship Motions". *Journal of Ship Research*, 47(3), pp. 208–221.
- [11] Peric, M., Zorn, T., el Moctar, O., Schellin, E., and Kim, Y., 2007. "Simulation of Sloshing in LNG-tanks". In 26th International Conference on Offshore Mechanics and Arctic Engineering. OMAE2007-29555.